Binder-enhanced reversible photochromic films by tungsten oxide hybrid composites for advanced applications

Min Sung Kim[1,a], Jun Ho Yoon[1,a], Hyun Kyu Lee[a], Tamaki Hirose[b], Yoshihiko Takeda[b,*], Jae Pil Kim[a,*]

[a]*Lab of Organic Photo-functional Materials, Department of Materials Science and Engineering, Seoul National University, 1 Gwanak-ro, Gwanak-gu, Seoul 08826, Republic of Korea*

[b]*Hydrogen Related Materials Group, Research Center for Energy and Environmental Materials, National Institute for Materials Science (NIMS), Tsukuba, Japan*

** Corresponding author.*

[1] *These authors contributed equally to this work.*

E-mails: jaepil@snu.ac.kr

Abstract

In this study, we developed binder-enhanced reversible photochromic tungsten oxide (WO_3) films for advanced applications. Expanding on previous research, we used tungsten oxide hybrid composites as the base material and incorporated various binders, specifically polyethylene glycol (PEG), polysorbate 80 (PS 80), and carboxymethyl cellulose (CMC), to evaluate their effects on reversible photochromic reactions. Our experiments demonstrated that the inclusion of CMC significantly improved the photochromic properties and exhibited the fastest reversible reactions when compared to PEG and polysorbate 80. This enhancement is attributed to the high density of hydroxyl groups and the network structure of CMC, which facilitate efficient proton transfer and oxygen permeability, both crucial for the reoxidation process in WO_3. Density functional theory (DFT) calculations supported these findings by indicating that CMC has a suitable bandgap and electron mobility, which enhance charge injection and transport. Additionally, the fabricated films showed consistent and stable performance under both heat treatment and natural ambient conditions. These results underscore the potential of CMC as an effective binder for developing high-performance, reversible photochromic films suitable for applications in smart windows, displays, and optoelectronic devices.

1. Introduction

Photochromism, the phenomenon where materials undergo reversible color or transmittance changes in response to light, is pivotal for applications in smart windows, displays, and optoelectronic devices [1, 2]. Among various photochromic materials, tungsten oxide (WO_3) stands out for its stability and ease of synthesis [3, 4]. However, its narrow bandgap (2.7–2.8 eV) facilitates electron-hole recombination, resulting in inefficient performance [2, 4-6].

In our previous study [7], we explored the fundamental photochromic properties of tungsten oxide-based materials. Due to the similar nature of the WO_3 base material used in both studies, there are comparable analyses and results. However, a significant limitation in the previous study was the inefficiency of the bleaching process. While we observed the color change, the reverse reaction, or bleaching reaction, did not proceed effectively. Attempts to induce natural bleaching in the ambient condition over 20 hours were unsuccessful, with complete bleaching process not achieved and the process being excessively prolonged. This limitation highlights a critical challenge in achieving efficient reversible reactions in photochromic films.

To address these limitations, various strategies have been proposed. These include incorporating diverse metal elements, maximizing surface area through the formation of quantum dot structures, introducing organic compounds, and inducing structural modifications [2, 3, 5, 6]. For instance, Zhang et al. developed WO_3@poly (N-isopropyl acrylamide) hybrid spheres, where the amide groups in PNIPAM (poly(N-isopropylacrylamide)) assist in electron injection during the photochromic process [8]. Similarly, Dong et al. created a photochromic coating by combining amorphous WO_3-modified palygorskite (PAL) nanorods with polysiloxane, which acts as an electron donor to increase the bleaching speed of the coating while also imparting superhydrophobic properties [9].

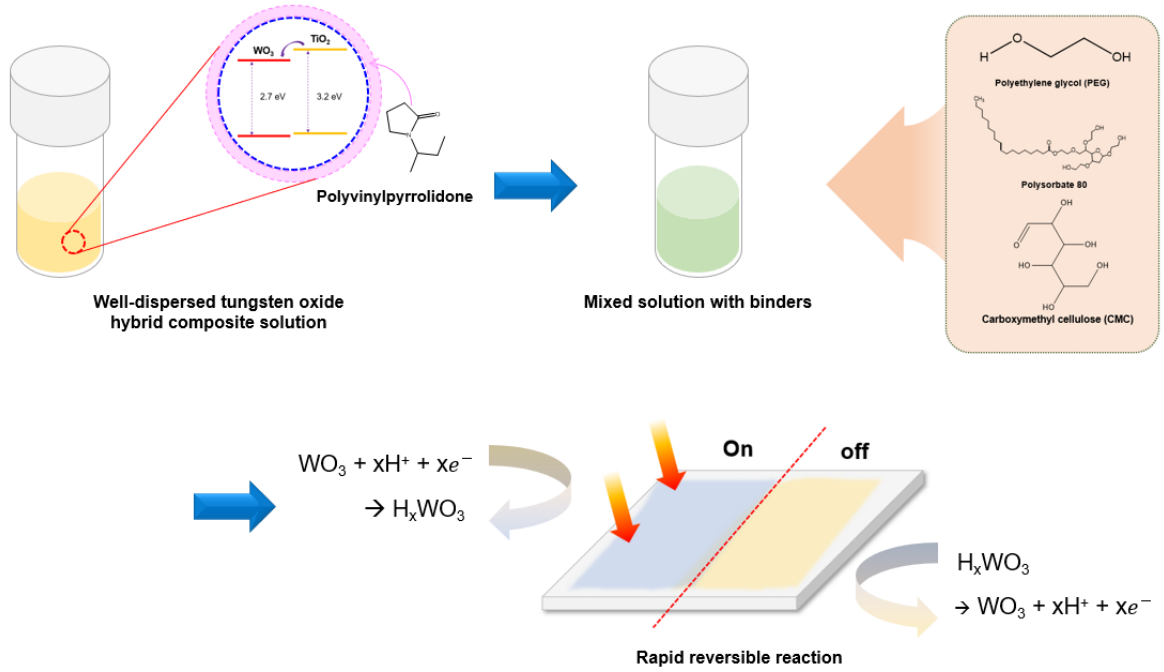
Enhancing the coloration process in WO_3, which depends on the formation of W^{5+}, can also be achieved by increasing the concentration of oxygen vacancies within the stabilized crystal structure [4, 6, 10]. Oxygen-deficient WO_3 quantum dots, for example, have been shown to enhance photochromic performance. Additionally, doping WO_3 with other elements can further improve its properties. Dong et al. demonstrated that doping h-WO_3 with an appropriate amount of Cu promotes carrier separation through interfacial charge transfer (IFCT), thereby enhancing the coloration efficiency [11].

To augment the photochromic properties of WO_3, we incorporated titanium oxide (TiO_2), a well-known photocatalyst capable of injecting electrons into WO_3 upon light irradiation [12-14]. Our experiments determined that a 3% molar ratio of TiO_2 provided optimal enhancement in photochromic performance, as confirmed by TEM, XRD, and reflectance measurements.

For the fabrication of photochromic films, we employed the doctor blade method, a solution-based technique suitable for large-scale production. The challenge of dispersing metal oxides in organic solvents was addressed by using polyvinylpyrrolidone (PVP) as a dispersant. Our previous research demonstrated that PVP not only improves dispersion through the ligand-to-metal charge transfer (LMCT) effect but also enhances the photochromic properties of WO_3.

Furthermore, we evaluated various binders, including polyethylene glycol (PEG), polysorbate 80 (PS 80), and carboxymethyl cellulose (CMC), to enhance the reversible performance of tungsten oxide hybrid composites. Our study reveals that CMC offers a unique combination of structural advantages, including a high density of hydroxyl groups and a network structure that facilitates efficient oxygen diffusion. These properties enable rapid reverse reactions and enhance the overall photochromic performance, as supported by density functional theory (DFT) calculations.

This research demonstrates the potential for developing practical photochromic films with efficient reversible reactions by incorporating binders like CMC. The findings highlight the importance of selecting binders with structural characteristics that improve oxygen permeability and proton transfer, paving the way for advanced applications in smart windows, displays, and optoelectronic devices.



Scheme 1. The overall process of introducing various binders in tungsten oxide hybrid composites

2. Experimental section

2.1. Materials

Ammonium tungstate pentahydrate (ATP, $5(NH_4)_2O{\cdot}12WO_3{\cdot}5H_2O$), polyvinylpyrrolidone (PVP, $(C_6H_9NO)_n$), and oxalic acid (anhydrous, 98%) were acquired from Alfa Aesar. Ethyl alcohol (extra pure, 99.5%), PGME (extra pure, 1-Methoxy-2-propanol, 98.5%), and TiO_2 (P25) were purchased from SAMCHUN Pure Chemical CO., LTD. Polysorbate 80 and carboxymethyl cellulose were obtained from Alfa Aesar. Polyethylene glycol was purchased from Tokyo Chemical Industry Co., LTD. Also, Distilled water(pure water, 100%) was purchased from SAMCHUN Pure Chemical CO., LTD. All the reagents were used without any additional purification.

2.2. Preparation of WO_3 nanoparticles

WO_3 nanoparticles were synthesized via a hydrothermal technique. The synthesis process is detailed as follows: A reactor with a 150 mL capacity was used. Initially, 15.6 g of ATP was mixed into 70 mL of distilled water within a beaker. Then, 20 mL of oxalic acid solution was added to the mixture with constant stirring. Oxalic acid solution

was prepared by dissolving 10 g of oxalic acid in 100 mL of deionized water. The pH of the resulting solution was adjusted to 1.0 through the addition of 2M HCl. This mixture was stirred continuously for 4 hours before being transferred to the reactor. The reaction mixture was then subjected to heating at 120 °C for 12 hours. Post-reaction, the resultant tungsten oxide was harvested by centrifugation. The collected precipitate was thoroughly washed with ethanol to obtain the final product.

2.3. Synthesis of the composite

After the synthesis of the nanoparticle composite, it underwent two washes with deionized water and ethanol. Then, TiO_2 was added in molar ratios of 3% and stirred for 3 hours. Polyvinylpyrrolidone was added to the tungsten oxide ethanol mixture at 50 wt%, followed by stirring for 1 hour and ultrasonication for 30 minutes. The process ended after 12 hours of stirring. The final product was centrifuged and washed with 1-methoxy-2-propanol (PGME), and then combined with a solvent containing 20 wt% PGME to create a dispersed solution.

2.4. Fabrication of photochromic film

A glass slide (2×2 cm) was cleaned with nitrogen gas. A solution of 30 wt% tungsten oxide in PGME was mixed with 20 wt% acrylate binder in a 3:2 ratio and stirred at room temperature for 24 hours. Polysorbate 80 was mixed with the tungsten oxide solution at a mass ratio of 1:3 wt% and stirred. CMC and PEG were dissolved in D.I. water at concentrations of 10 wt% and 20 wt%, respectively, and stirred for one hour to ensure complete dissolution. Afterward, these solutions were mixed with the tungsten oxide solution at a mass ratio of 1:3 wt% and stirred for one hour. All mixed solutions were subsequently drop-casted onto the glass slide and coated using a doctor blade technique. The sample was then heated at 100 °C for 2 minutes to evaporate any residual solvent.

2.5. Characterization and measurement

High-resolution X-ray diffraction (HRXRD) analysis of the coated film was performed using a SmartLab system equipped with Cu-Kα radiation (λ = 0.154 nm). Field emission transmission electron microscopy (FE-TEM)

images were acquired using a JEOL JEM-F200 instrument. Field emission scanning electron microscopy (FE-SEM) images were obtained using a JEOL JSM-7800F Prime instrument, with a platinum coating applied via a Zeiss MERLIN Compact. UV-Vis reflectance spectra were measured using a JASCO V-770 spectrophotometer. Fourier-transform infrared (FT-IR) spectroscopy was performed with a Bruker TENSOR27 spectrometer. UV-Vis transmittance spectra were acquired using a Perkin Elmer Lambda 1050 spectrophotometer. Dynamic light scattering (DLS) measurements were carried out with a DLS-8000HAL from Photal Otsuka Electronics. Zeta potential measurements were performed with an ELSZ-1000 from Photal Otsuka Electronics, with 1-minute measurement intervals and auto-correlation function fitting using Anton Paar's Kalliope software. Thermogravimetric analysis (TGA) was carried out using a heating rate of 10 °C/min using a TA Instruments SDT Q600. X-ray photoelectron spectroscopy (XPS) was conducted using a Thermo Fisher Scientific Sigma Probe for electron spectroscopy chemical analysis.

2.6. Density functional theory (DFT) calculation

The geometry optimization of PEG, polysorbate 80, and CMC was calculated on the basis of the B3LYP/6-31G(d,p) level. All calculations were carried out using Gaussian 16 software.

3. Results and Discussion

3.1 Characterization of the tungsten oxide hybrid composite

This study builds upon previous research, specifically doi:10.1016/j.colsurfa.2024.134083, by continuing the investigation of tungsten oxide hybrid composites [7]. Using similar materials and methods, we synthesized tungsten oxide (WO_3) through a sol-gel method, achieving a hexagonal structure as confirmed by X-ray diffraction (XRD) analysis (Fig. 1(a)). The hexagonal structure provides a larger surface area compared to the monoclinic structure, enhancing reactivity and photochromic properties (Fig. S1) [15-17].

SEM and TEM analyses were conducted to examine the morphology and confirm the structure. SEM images revealed particle clustering with sizes ranging from a few hundred nanometers to several micrometers. TEM images showed a plate-like morphology with dimensions of approximately 10 nm in width and 40 nm in length.

Lattice parameters measured by TEM, 0.67 nm for the (100) plane and 0.35 nm for the (002) plane, validated the hexagonal structure (Fig. S2) [18, 19].

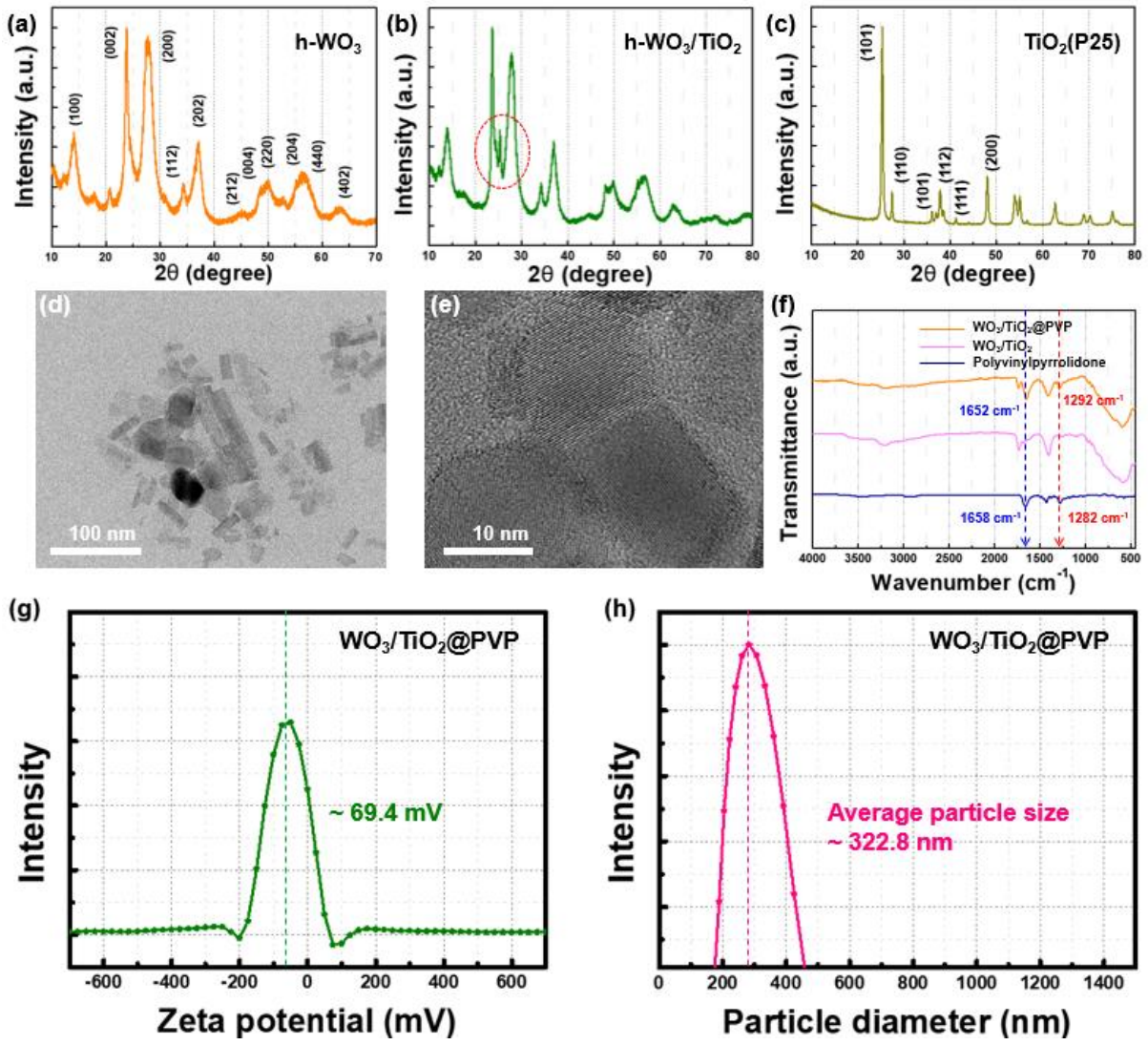


Fig. 1. XRD patterns of (a) hexagonal tungsten oxide, (b) tungsten oxide/titanium oxide composite, and (c) titanium oxide (P25). (d) High-magnification TEM image of composite and (e) HRTEM image of the composite. (f) FT-IR analysis of tungsten oxide hybrid composite. (g) Zeta potential and (h) DLS analysis of the tungsten oxide hybrid composite.

FT-IR spectroscopy and XPS analysis were employed to verify the bonding characteristics and oxidation states. FT-IR spectra indicated the presence of characteristic W-O-W vibrations and intercalated water molecules (Fig. 1(f)). XPS analysis confirmed the formation of a 6+ oxidation state, with notable peaks corresponding to W^{6+} and

W^{5+} (Fig. S3) [20].

To address the rapid recombination of photo-generated electron-hole pairs, TiO_2 was adsorbed onto the tungsten oxide surface. XRD patterns and TEM images confirmed the presence and physical adsorption of TiO_2 (Fig. 1(b), (d), and (e)) [21, 22]. Additionally, FT-IR analysis indicated successful adsorption of PVP onto the composite surface through hydrogen bonding. Moreover, TGA analysis revealed that the tungsten oxide has a hexagonal structure and contains approximately 7.5% hydrate (Fig. S4).

The reflectance measurement results showed that the tungsten oxide and titanium oxide composite exhibited a 14% higher change rate compared to previous research findings [23]. This improvement can be attributed to minimizing the rapid recombination caused by the small bandgap of tungsten oxide and enhancing photochromic properties through charge injection from titanium oxide to tungsten oxide (Fig. S5).

Finally, dispersibility analysis in organic solvent was conducted using zeta potential and DLS measurements. The introduction of PVP significantly increased the zeta potential, indicating stable dispersion, with a measured value of 69.4 mV, confirming a stable dispersed state (Fig. 1(g), Fig. S6(a)). DLS analysis further confirmed improved dispersion with reduced particle sizes and narrower distribution widths (Fig. 1(h), Fig. S6(b)).

In summary, by utilizing similar materials and methods as those in doi:10.1016/j.colsurfa.2024.134083 and doi:10.3390/nano14131121, we successfully synthesized and characterized a tungsten oxide hybrid composite. The incorporation of titanium oxide and PVP enhanced the photochromic properties and dispersion stability, resulting in a well-dispersed tungsten oxide hybrid composite solution with improved characteristics.

3.2 Reversible reaction in photochromic mechanism

Following the characterization results, we further investigated the photochromic mechanisms of the synthesized tungsten oxide hybrid composite. Understanding both the forward and reverse reactions is crucial for developing efficient and durable photochromic materials. The forward reaction in WO_3 photochromism involves the absorption of light, leading to electron-hole pair generation, followed by the reduction of tungsten ions and subsequent color change [2, 4, 20, 24]. Conversely, the reverse reaction involves the re-oxidation of tungsten ions and the restoration of the material to its original colorless state.

When exposed to UV or visible light, WO_3 absorbs photons, leading to the excitation of electrons from the

valence band to the conduction band. This process creates electron-hole pairs [3, 24, 25]:

$$WO_3 + h\nu \rightarrow e^- + h^+ \quad (1)$$

These photogenerated electrons are then trapped by tungsten ions (W^{6+}), reducing them to W^{5+} and leading to the formation of tungsten bronze (H_xWO_3). This process is accompanied by the injection of protons (H^+) into the WO_3 structure:

$$WO_3 + xH^+ + xe^- \rightarrow H_xWO_3 \quad (2)$$

The reduced form (W^{5+}) of tungsten and the incorporation of protons induces a visible color change, typically to blue, which is the hallmark of the photochromic effect in WO_3.

The reverse reaction is fundamentally the reoxidation process, where W^{5+} is oxidized back to W^{6+}, and the protons are removed from the WO_3 lattice, restoring its original colorless state:

$$H_xWO_3 \rightarrow WO_3 + xH^+ + xe^- \quad (3)$$

This process typically requires the presence of oxygen or another suitable oxidizing agent to facilitate the electron removal:

$$W^{5+} + \frac{1}{2}O_2 \rightarrow W^{6+} + e^- \quad (4)$$

The reverse reaction in WO_3-based photochromic systems is often less efficient and slower than the forward reaction. Several factors contribute to these challenges. Firstly, the recombination of photogenerated electron-hole pairs in WO_3 is inherently slow due to the relatively narrow bandgap (2.7–2.8 eV) and the strong trapping of electrons by W^{6+} ions [2, 6, 26]. This results in prolonged retention of the colored state, as observed in various studies. Additionally, efficient reverse reactions depend on the availability and diffusion of oxygen within the material. The rate of oxygen diffusion can be hindered by the dense WO_3 lattice or inadequate surface exposure, limiting the reoxidation process [27, 28]. Structural integrity and hydration state of WO_3 also play critical roles. Hydrated forms of WO_3, such as $H_xWO_3 \cdot nH_2O$, can facilitate proton diffusion and reoxidation. However, the loss of structural stability or changes in hydration levels can impede the reverse reaction. Furthermore, surface adsorption of species such as PVP can influence the availability of active sites for oxygen adsorption and electron exchange [7, 29, 30]. While PVP enhances dispersion and photochromic properties through LMCT effects, it can also create steric hindrance [31].

To address these limitations, we introduced PEG, polysorbate 80, and CMC binders, which are expected to

influence reversible reactions in different ways. These binders are anticipated to affect the photochromic performance by enhancing proton mobility, facilitating oxygen diffusion, and improving the structural stability of the composite material.

3.3 Introduction of various binders for reversible reactions

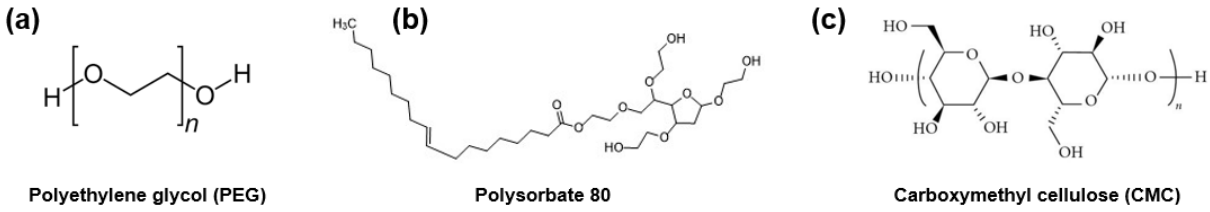


Fig. 2. The types of introduced binders. (a) polyethylene glycol (PEG), (b) polysorbate 80, and (c) carboxymethyl cellulose (CMC).

To address these limitations and further improve the reversible reactions in WO_3-based photochromic systems, we introduced three different binders: PEG, polysorbate 80, and CMC. These binders were selected based on their unique chemical properties, which are expected to enhance the efficiency of the reverse reactions by facilitating proton mobility, improving oxygen diffusion, and stabilizing the composite structure (Fig. 2) [32-37].

PEG is a hydrophilic polymer known for its ability to improve the dispersion of nanoparticles in a solvent and enhance proton conductivity [32, 33]. PEG contains numerous ether groups (-C-O-C-), which can potentially facilitate the mobility of protons through hydrogen bonding [38]. This characteristic can be beneficial in improving the reverse reaction mechanism in WO_3 by enhancing proton transfer within the material. However, the relatively low density of -OH groups in PEG might limit its effectiveness in facilitating the required proton supply for the reverse reactions. Despite its potential benefits, PEG's impact on the overall efficiency of the reversible reactions in WO_3 photochromism may be limited.

polysorbate 80 is a surfactant characterized by a lengthy hydrophobic tail and a hydrophilic head group, known for its ability to enhance the dispersion of hydrophobic particles in aqueous solutions [34, 35]. Polysorbate 80 can introduce additional electron donor sites through its oxygen-rich structure, potentially aiding in the electron transfer processes [39]. However, DFT calculations suggest that the electron orbitals in polysorbate 80 are confined within its long molecular chains, which might impede the efficient transfer of electrons to the WO_3

surface (Fig. S8). Moreover, the long hydrophobic chains could potentially hinder the interaction between WO_3 and the surrounding oxygen, thus reducing the overall effectiveness of the reverse reactions. This suggests that while polysorbate 80 can aid in dispersion, its long molecular structure might limit its effectiveness in enhancing reversible photochromic reactions.

CMC is a polysaccharide derivative with a high density of hydroxyl (-OH) groups along its polymer backbone [36, 37]. This characteristic makes CMC an excellent candidate for facilitating proton mobility and enhancing the reverse reactions in WO_3 photochromic systems. The high density of -OH groups can provide a continuous supply of protons necessary for the reoxidation of W^{5+} back to W^{6+}, thereby improving the efficiency of the reverse reaction [40]. Additionally, CMC's network structure can enhance oxygen permeability, facilitating better oxygen diffusion to the WO_3 surface and thereby supporting the reoxidation process. DFT calculations also support the suitability of CMC, indicating that its bandgap and electron mobility are favorable for electron transfer processes (Fig. 3). These properties suggest that CMC is likely the most effective binder among the three for enhancing the reversible reactions in WO_3 photochromic systems.

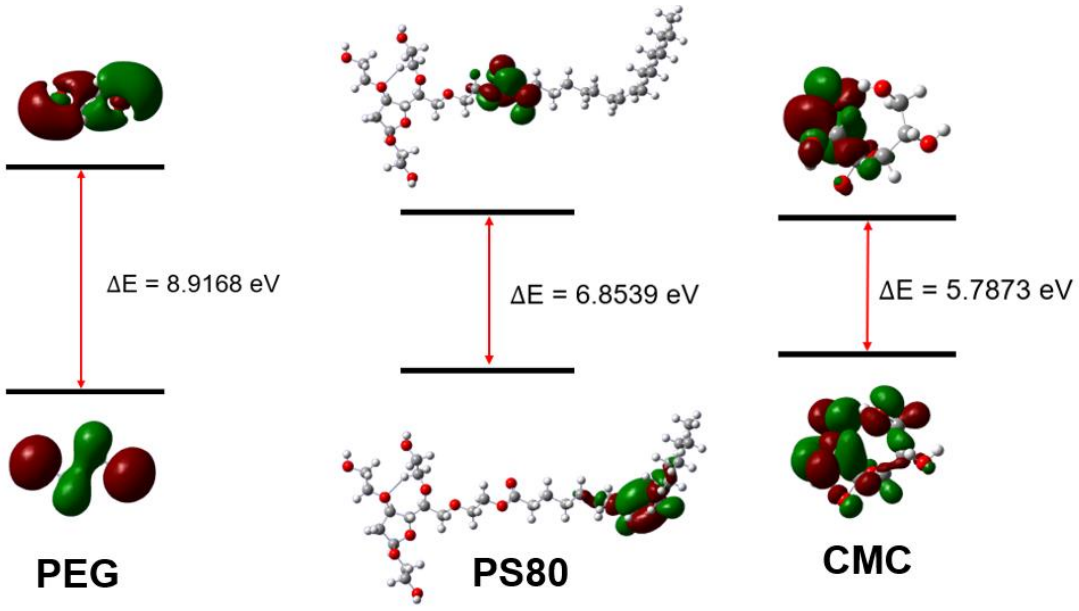


Fig. 3. DFT calculations were performed using the B3LYP/6-31G(d,p) basis set for geometry optimization. The band gap of PEG is 8.9169 eV, PS 80 is 6.8539 eV, and CMC is 5.7873 eV.

3.4 Reversible photochromic films by heat treatment

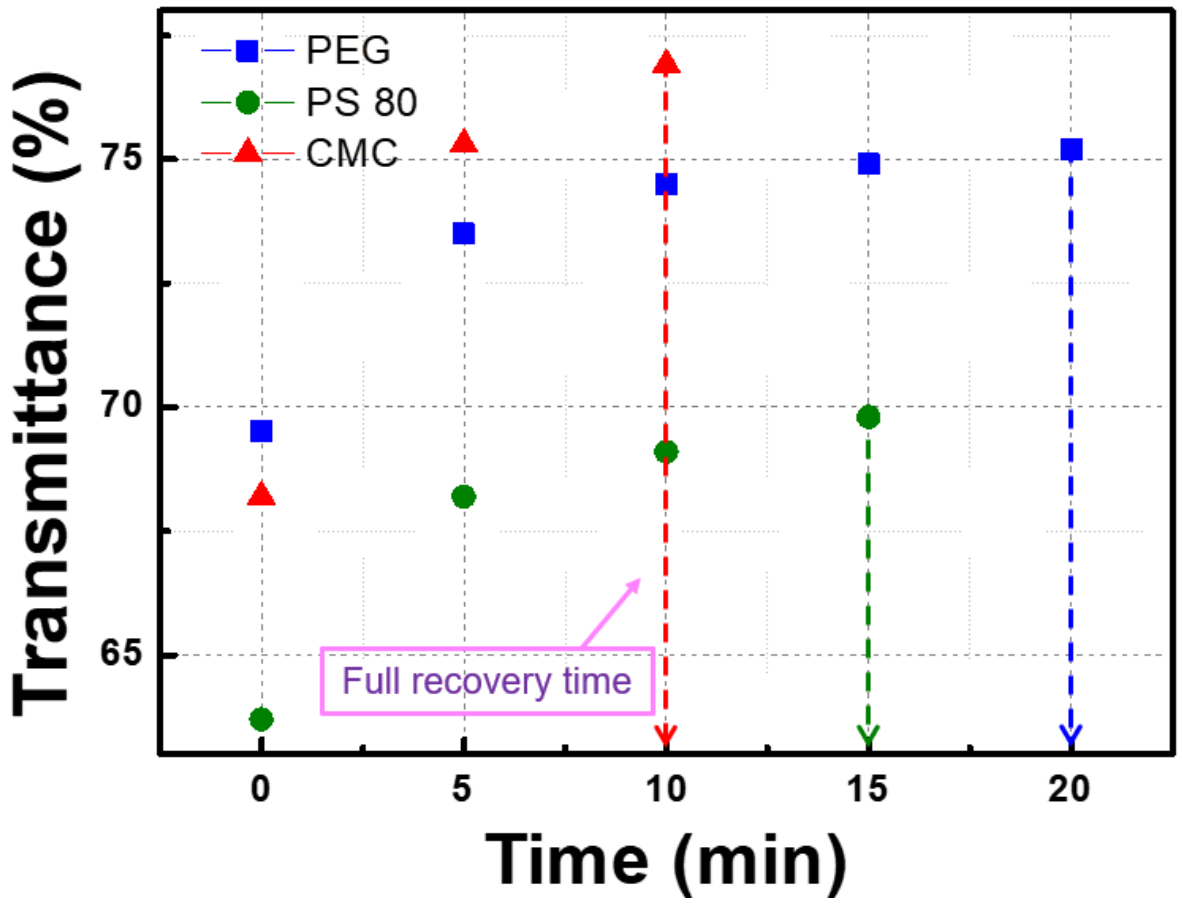


Fig. 4. The time required to fully return to the original color after 1 minute of UV irradiation. For the CMC-based film, it took 10 minutes. For the PS 80-based film, it took 15 minutes. For the PEG-based film, it took 20 minutes.

Table 1

The bleaching time with heating at 60°C. After 1 minute of UV irradiation to induce photochromic reaction, the time required for complete bleaching process was measured at 5-minute intervals.

Time	Pristine	UV 1min	Heat 5min	Heat 10min	Heat 15 min	Heat 20min
PEG	75.4	69.5	73.5	74.5	74.9	75.0
Polysorbate 80	70.0	63.7	68.2	69.1	69.8	-
CMC	77.1	68.2	75.3	76.9	-	-

Based on the previous mechanism, we first examined the speed of the reverse reaction by measuring the reverse process under heat treatment. Since the standard heat treatment temperature for tungsten oxide is typically set at 60°C, we fixed the heating temperature at 60°C in this study to observe the reaction. The experimental procedure

involved exposing the films to UV light for 1 minute to induce a color change, followed by heat treatment at approximately 60°C. The bleaching progress was observed at 5-minute intervals for up to 20 minutes (Fig. 4). Additionally, to minimize excessive variations in characteristics and to uniformly adjust the amount of tungsten oxide hybrid composite, films were prepared with a similar thickness of approximately 4–5μm for measurement (Fig. S7).

The results indicate significant differences in the bleaching efficiency among the films with different binders. The PEG-based film showed approximately 90% recovery of its original transmittance after 20 minutes of heat treatment, achieving complete bleaching after 30 minutes. The polysorbate 80-based film demonstrated faster recovery, with about 90% recovery after 10 minutes and complete bleaching at 15 minutes. Remarkably, the CMC-based film exhibited the most rapid response, with approximately 90% recovery within 5 minutes and complete bleaching after 10 minutes of heating (Table 1).

These observations suggest that the choice of binder significantly influences the heat-induced bleaching efficiency of tungsten oxide-based photochromic films. The superior performance of the CMC-based film can be attributed to several key factors. Firstly, CMC contains a high density of hydroxyl (-OH) groups along its polymer backbone. These -OH groups facilitate proton transfer, which is crucial for the reoxidation of W^{5+} to W^{6+} during the reverse reaction. The continuous supply of protons from the -OH groups in CMC aids in maintaining the efficiency of the reverse reaction. Secondly, the network structure of CMC enhances the permeability of oxygen, which is essential for the reoxidation process. Improved oxygen diffusion to the WO_3 surface supports the conversion of W^{5+} back to W^{6+}, thereby accelerating the reverse reaction. Previous studies have shown that enhanced oxygen permeability can significantly improve the reoxidation kinetics in photochromic materials. Thirdly, DFT calculations indicate that CMC has a suitable bandgap and electron mobility, which are beneficial for electron transfer processes. The presence of CMC likely facilitates more efficient electron removal and reoxidation of tungsten ions. The suitable electronic properties of CMC support efficient charge transport, which is critical for the rapid recovery of the initial state. Uniform dispersion and enhanced structural integrity contribute to consistent and repeatable photochromic responses, as observed in the heat treatment experiments.

3.5 Naturally reversible light-responsive photochromic film

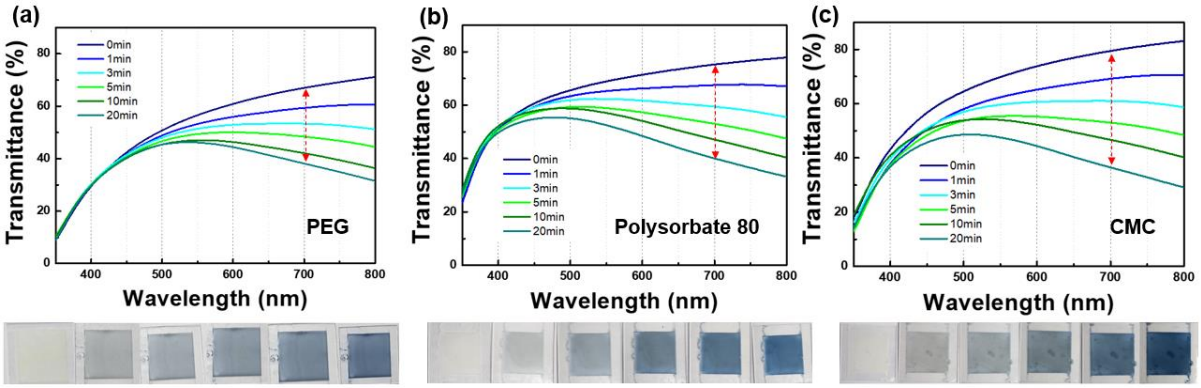


Fig. 5. The transmittance of the photochromic film over time. The maximum coloration time is 20 min.

Table 2

The transmittance of the photochromic film over time (% at 700nm wavelength)

Time	0min	1min	3min	5min	10min	20min	△T (%)
PEG	67.0	59.4	53.3	48.4	42.1	38.2	**28.8**
Polysorbate 80	75.3	67.5	59.4	53.0	47.1	40.1	**35.2**
CMC	79.5	69.2	61.0	53.0	46.7	36.5	**43.0**

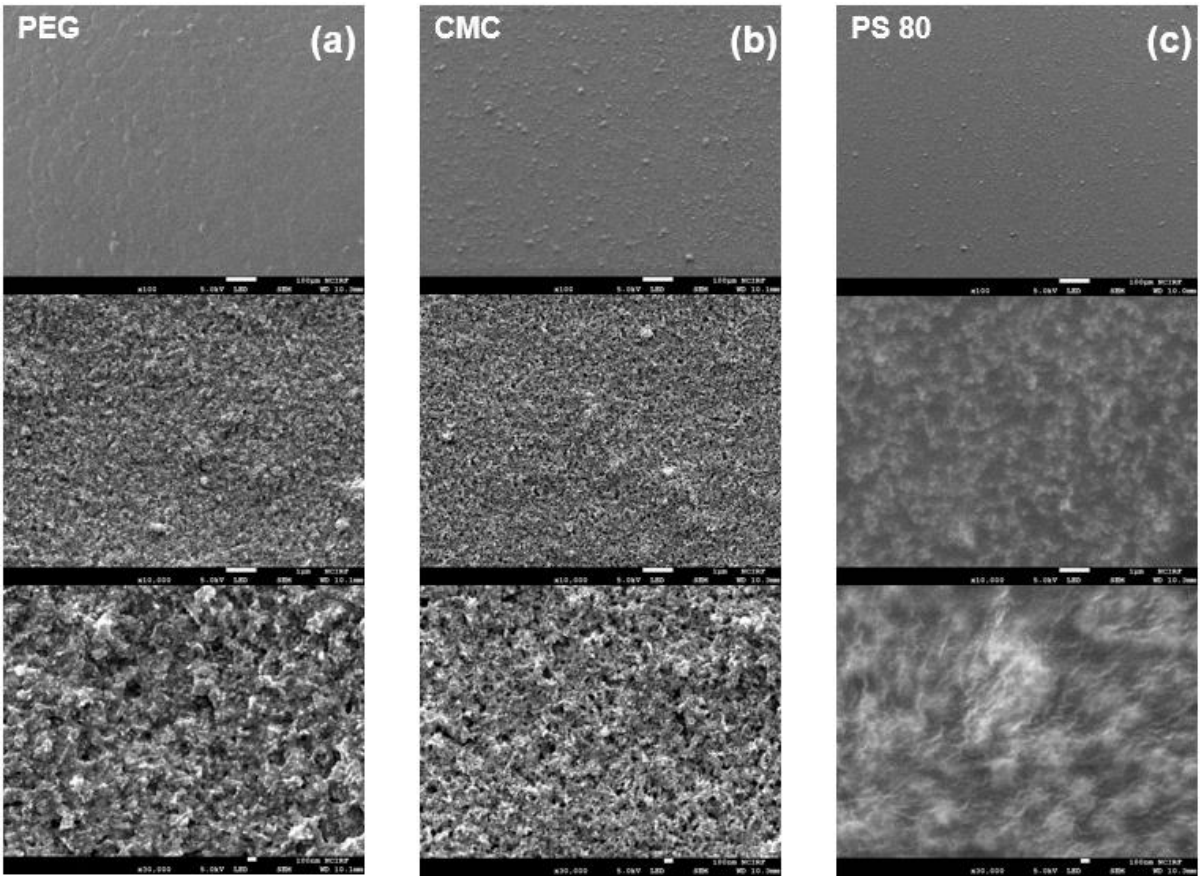


Fig. 6. SEM images of introducing various binders. (a) PEG, (b) CMC, and (c) PS 80.

Based on the previous results, we ultimately measured the efficiency of the reversible reaction under natural ambient conditions without applying heat. To achieve this, we observed the reverse reaction at room temperature. Using the tungsten oxide hybrid composite solution, we fabricated films via the doctor blade method to examine their photochromic properties (Fig. 5). To investigate the morphology of the fabricated films, we conducted SEM measurements. Although some surface undulations were observed, no cracks or pores were detected (Fig. 6). The transmittance data of the films over different time intervals during UV irradiation are shown in Table 2. The change in transmittance (ΔT) was calculated for each binder. The data indicate that the CMC-based film exhibits the highest transmittance change (ΔT) of 43.0%, suggesting superior photochromic performance compared to PEG (28.8%) and polysorbate 80 (35.2%). The film made with the CMC binder exhibited the best performance, demonstrating superior properties compared to traditional films and previous research results. This can be attributed to CMC's ability to supply the necessary protons for the photochromic mechanism, enhancing charge injection and thereby improving the photochromic properties.

Also, we present the results of photochromic properties and cycle tests of tungsten oxide-based films using various binders: PEG, polysorbate 80, and CMC. The films were subjected to UV irradiation for 1 minute followed by bleaching process for 30 minutes. Although the bleaching time might seem short and the change rate modest, the observed rapid reverse reaction speed is notable for films, compared to previous studies conducted on powder or liquid states. The cycle test results, as depicted in Fig. 7, further demonstrate the efficiency of the CMC-based film. The test involved exposing the films to UV light for 1 minute followed by a 30-minute bleaching period, repeated over multiple cycles. The CMC-based film (WTP@CMC) consistently shows higher transmittance recovery and stability over multiple cycles compared to the films with PEG (WTP@PEG) and polysorbate 80 (WTP@PS 80). Also, as shown in Table 3, after approximately seven repeated tests, the other binders show differences of about 9.0% and 6.2% between the initial and final cycle tests compared to the pristine state, indicating incomplete recovery. In contrast, when using the CMC binder, the difference is only about 0.1% from the initial state, confirming that reversible reactions occur actively. These results indicate a fast reversible reaction compared to previous findings, even without additional heat treatment (Table 4).

To summarize, the introduction of CMC as a binder significantly enhances the photochromic properties and reverse reaction speed in tungsten oxide-based films. The high density of hydroxyl groups, improved oxygen permeability, favorable electron transfer characteristics, and enhanced structural stability contribute to the superior performance of the CMC-based film. These findings highlight the potential of CMC as an effective binder for developing advanced photochromic materials with rapid and efficient reversible reactions.

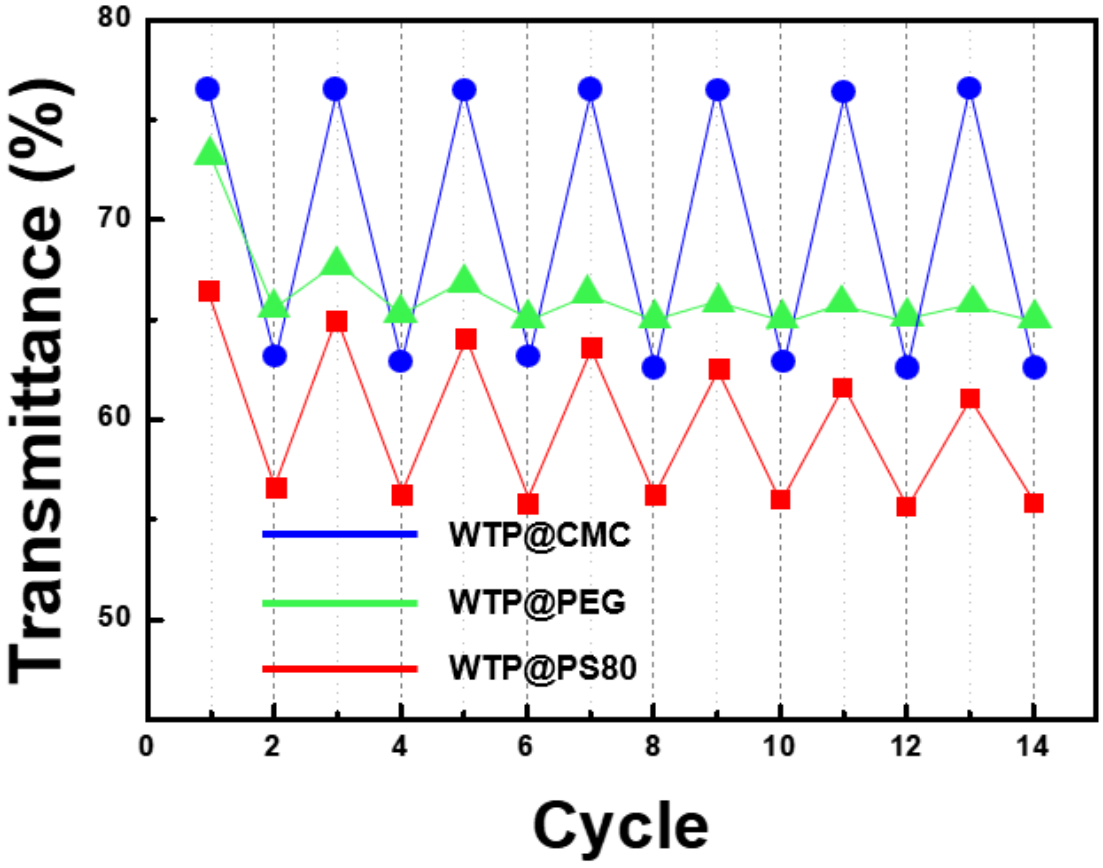


Fig. 7. The change of transmittance at 700 nm for 14 switching cycles of each film by different binders.

Table 3

The cycle test of each film. (% at 700nm wavelength)

Time	PEG	Polysorbate 80	CMC
Pristine state	73.8	67.1	77.2
1	65.9	56.7	63.0
off	68.1	64.9	77.0
2	65.6	55.8	62.8
off	67.4	64.0	76.5
3	64.9	55.4	63.1
off	65.2	63.8	77.0
4	64.5	55.0	61.9
off	65.0	62.5	76.3
5	63.8	54.8	62.5
off	64.9	62.0	76.8
6	64.0	55.0	62.2
off	65.0	61.8	76.9
7	63.8	55.2	62.3
Off	64.8	60.9	77.1
△T (%) at 0 to end	**9.0**	**6.2**	**0.1**

Table 4

Comparison of previously reported and this study's reversibility in photochromic films [41].

sample	UV irradiation conditions	Irradiation time	Reversibility	Ref
Mo/WO_3	-	120 min	-	[42]
$YHx:O/WO_3$	-	10 min	<1 h at 60 ℃	[43]
WO_3/PC	Sunlight	40 min	Air/72 h	[44]
$WO_3•H_2O$/PVA	365 nm, 8W	5 min	Air/dark 3 d	[45]
WO_{3-x}/Ta_2O_5	365 nm, 8W	10 sec	-	[46]
WO_3/PU/PVP	-	< 5 min	<1 h at 60 ℃	[47]
WO_3/PVP (previous work)	365 nm, 8W	20 min	Air/Dark 24 h (no recovery)	[7]
WO_3/TiO_2@PVP with CMC binder	365 nm, 8W	1min	10 min at 60 ℃	In this work
	365 nm, 8W	1 min	30 min	

4. Conclusion

In this study, we introduced various binders to create structures that allow for better oxygen diffusion and enhance proton donation through numerous hydroxyl (-OH) groups, thereby improving reversible reactions. Based on these improvements, we fabricated photochromic films and analyzed their properties and decolorization reactions. We selected four binders based on their structural features and the number of OH groups. The results of the forward photochromic reaction measurements showed that carboxymethyl cellulose (CMC), with the highest number of OH groups, exhibited the greatest change in transmittance. Additionally, when analyzing the reverse reaction through heating, CMC demonstrated the fastest recovery time of approximately 10 minutes. Finally, during the cycle tests conducted at room temperature without heating, CMC consistently showed effective reversible reactions, with near-complete recovery even after repeated testing. Our findings confirm that oxygen diffusion and proton mobility are critical factors in the reverse reaction mechanism, which are closely related to the

structural properties of CMC. CMC's network structure facilitates better oxygen penetration and, due to its abundant OH groups, allows for easy proton mobility, making it an advantageous material for reversible reactions. The results of this study demonstrate that if a material structurally enables efficient oxygen diffusion and proton mobility, such as CMC, it can significantly contribute to the practical application and development of high-performance photochromic films utilizing tungsten oxide, thereby advancing related research.

Acknowledge

This work was supported by Ministry of Trade, Industry and Energy (Grant No. 20010838) and the International Cooperative Graduate Program, National Institute for Materials Science (NIMS). We would like to express my gratitude to Dr. Isaka Noriko for her assistance in facilitating TEM analysis. Additionally, I extend my thanks to Dr. Hattori Shinya and Ms. Maruhashi Keiko for their support and guidance during the initial measurements and learning processes with the equipment. The Institute of Engineering Research at Seoul National University also provided research facilities for this work. We also thank the staff and crew of National Center for Inter-University Research Facilities (NCIRF, RIAM) of Seoul National University for assistance with XRD, TEM, FESEM, XPS, UV-vis spectroscopy measurements.

References

[1] S.K. Deb, Optical and photoelectric properties and colour centres in thin films of tungsten oxide, Philosophical Magazine, 27 (2006) 801-822.
[2] S. Wang, W. Fan, Z. Liu, A. Yu, X. Jiang, Advances on tungsten oxide based photochromic materials: strategies to improve their photochromic properties, Journal of Materials Chemistry C, 6 (2018) 191-212.
[3] X. Dong, Y. Lu, X. Liu, L. Zhang, Y. Tong, Nanostructured tungsten oxide as photochromic material for smart devices, energy conversion, and environmental remediation, Journal of Photochemistry and Photobiology C: Photochemistry Reviews, 53 (2022).
[4] S. Cong, F. Geng, Z. Zhao, Tungsten Oxide Materials for Optoelectronic Applications, Adv Mater, 28 (2016) 10518-10528.
[5] X. Zhang, Y. Wei, R. Yu, Multidimensional Tungsten Oxides for Efficient Solar Energy Conversion,

Small Structures, 3 (2021).
[6] M. Ataalla, A.S. Afify, M. Hassan, M. Abdallah, M. Milanova, H.Y. Aboul-Enein, A. Mohamed, Tungsten-based glasses for photochromic, electrochromic, gas sensors, and related applications: A review, Journal of Non-Crystalline Solids, 491 (2018) 43-54.
[7] M.S. Kim, H.K. Lee, J.H. Yoon, H.M. Kim, Y.S. Kim, J.P. Kim, Improving dispersibility of tungsten oxide particles with organic ligands for photochromic films, Colloids and Surfaces A: Physicochemical and Engineering Aspects, (2024) 134083.
[8] Q. Zhang, R. Wang, Y. Lu, Y. Wu, J. Yuan, J. Liu, Highly efficient photochromic tungsten oxide@ PNIPAM composite spheres with a fast response, ACS Applied Materials & Interfaces, 13 (2021) 4220-4229.
[9] J. Dong, J. Zhang, Photochromic and super anti-wetting coatings based on natural nanoclays, Journal of materials chemistry A, 7 (2019) 3120-3127.
[10] Y. Badour, S. Danto, C. Labrugère, M. Duttine, M. Gaudon, Cu-doped and un-doped WO3 photochromic thin films, Journal of Electronic Materials, 51 (2022) 1555-1567.
[11] X. Dong, Z. Wu, Y. Guo, Y. Tong, X. Liu, L. Zhang, Y. Lu, Rational modification in the photochromic and self-bleaching performance of hierarchical microsphere Cu@ h-WO3/WO3· nH2O composites, Solar Energy Materials and Solar Cells, 219 (2021) 110784.
[12] P. Cheng, C. Deng, X. Dai, B. Li, D. Liu, J. Xu, Enhanced energy conversion efficiency of TiO2 electrode modified with WO3 in dye-sensitized solar cells, Journal of Photochemistry and Photobiology A: Chemistry, 195 (2008) 144-150.
[13] X. Sun, C. Wang, D. Su, G. Wang, Y. Zhong, Application of photocatalytic materials in sensors, Advanced Materials Technologies, 5 (2020) 1900993.
[14] K. Wang, Z. Wei, C. Colbeau-Justin, A. Nitta, E. Kowalska, P25 and its components-electronic properties and photocatalytic activities, Surfaces and Interfaces, 31 (2022) 102057.
[15] S. Shrestha, B. Wang, P. Dutta, Nanoparticle processing: Understanding and controlling aggregation, Advances in colloid and interface science, 279 (2020) 102162.
[16] Y. Zheng, G. Chen, Y. Yu, Y. Hu, Y. Feng, J. Sun, Urea-assisted synthesis of ultra-thin hexagonal tungsten trioxide photocatalyst sheets, Journal of Materials Science, 50 (2015) 8111-8119.
[17] W. Sun, M.T. Yeung, A.T. Lech, C.W. Lin, C. Lee, T. Li, X. Duan, J. Zhou, R.B. Kaner, High Surface Area Tunnels in Hexagonal WO(3), Nano Lett, 15 (2015) 4834-4838.
[18] R. Giannuzzi, V. Primiceri, R. Scarfiello, M. Pugliese, F. Mariano, A. Maggiore, C.T. Prontera, S. Carallo, C. De Vito, L. Carbone, V. Maiorano, Photochromic Textiles Based upon Aqueous Blends of Oxygen-Deficient WO3-x and TiO2 Nanocrystals, Textiles, 2 (2022) 382-394.
[19] M. S. Barbosa, F. M. B. Oliveira, X. Meng, F. Soavi, C. Santato, M. O. Orlandi, Tungsten oxide ion gel-gated transistors: how structural and electrochemical properties affect the doping mechanism, Journal of Materials Chemistry C, 6 (2018) 1980-1987.
[20] C. Guo, S. Yin, Q. Dong, T. Sato, Simple route to (NH4)(x)WO3 nanorods for near infrared absorption, Nanoscale, 4 (2012) 3394-3398.
[21] Y. Liao, J. Lin, B. Cui, G. Xie, S. Hu, Well-dispersed ultrasmall ruthenium on TiO2 (P25) for effective

photocatalytic N2 fixation in ambient condition, Journal of Photochemistry and Photobiology A: Chemistry, 387 (2020) 112100.
[22] Y. Liao, J. Qian, G. Xie, Q. Han, W. Dang, Y. Wang, L. Lv, S. Zhao, L. Luo, W. Zhang, 2D-layered Ti3C2 MXenes for promoted synthesis of NH3 on P25 photocatalysts, Applied Catalysis B: Environmental, 273 (2020) 119054.
[23] M.-S. Kim, J.-H. Yoon, H.-M. Kim, D.-J. Lee, T. Hirose, Y. Takeda, J.-P. Kim, Amplifying Photochromic Response in Tungsten Oxide Films with Titanium Oxide and Polyvinylpyrrolidone, Nanomaterials, 14 (2024) 1121.
[24] S. Zeb, G. Sun, Y. Nie, H. Xu, Y. Cui, X. Jiang, Advanced developments in nonstoichiometric tungsten oxides for electrochromic applications, Materials Advances, 2 (2021) 6839-6884.
[25] Y. Wang, X. Wang, Y. Xu, T. Chen, M. Liu, F. Niu, S. Wei, J. Liu, Simultaneous Synthesis of WO(3-)(x) Quantum Dots and Bundle-Like Nanowires Using a One-Pot Template-Free Solvothermal Strategy and Their Versatile Applications, Small, 13 (2017).
[26] F. Can, X. Courtois, D. Duprez, Tungsten-Based Catalysts for Environmental Applications, Catalysts, 11 (2021).
[27] J. Zhang, X. Chang, C. Li, A. Li, S. Liu, T. Wang, J. Gong, WO 3 photoanodes with controllable bulk and surface oxygen vacancies for photoelectrochemical water oxidation, Journal of Materials Chemistry A, 6 (2018) 3350-3354.
[28] Y. Liu, L. Kong, X. Guo, J. Xu, S. Shi, L. Li, Surface oxygen vacancies on WO3 nanoplate arrays induced by Ar plasma treatment for efficient photoelectrochemical water oxidation, Journal of Physics and Chemistry of Solids, 149 (2021) 109823.
[29] H.U. Khan, M. Tariq, M. Shah, S. Ullah, A.R. Ahsan, A. Rahim, J. Iqbal, R. Pasricha, I. Ismail, Designing and development of polyvinylpyrrolidone-tungsten trioxide (PVP-WO3) nanocomposite conducting film for highly sensitive, stable, and room temperature humidity sensing, Materials Science in Semiconductor Processing, 134 (2021).
[30] A.L. Popov, B. Han, A.M. Ermakov, I.V. Savintseva, O.N. Ermakova, N.R. Popova, A.B. Shcherbakov, T.O. Shekunova, O.S. Ivanova, D.A. Kozlov, A.E. Baranchikov, V.K. Ivanov, PVP-stabilized tungsten oxide nanoparticles: pH sensitive anti-cancer platform with high cytotoxicity, Mater Sci Eng C Mater Biol Appl, 108 (2020) 110494.
[31] O.L. Evdokimova, T.V. Kusova, O.S. Ivanova, A.B. Shcherbakov, K.E. Yorov, A.E. Baranchikov, A.V. Agafonov, V.K. Ivanov, Highly reversible photochromism in composite WO3/nanocellulose films, Cellulose, 26 (2019) 9095-9105.
[32] H. Chang, C. Lin, Proton conducting membranes based on PEG/SiO2 nanocomposites for direct methanol fuel cells, Journal of Membrane Science, 218 (2003) 295-306.
[33] M.E. Selvan, D.J. Keffer, S. Cui, Reactive molecular dynamics study of proton transport in polymer electrolyte membranes, The Journal of Physical Chemistry C, 115 (2011) 18835-18846.
[34] S.R. Hui, P. De Luna, How increasing proton and electron conduction benefits electrocatalytic CO2 reduction, Matter, 4 (2021) 1555-1577.
[35] E. Ha, W. Wang, Y.J. Wang, Peroxide formation in polysorbate 80 and protein stability, Journal

of pharmaceutical sciences, 91 (2002) 2252-2264.
[36] M. Saadiah, Y. Nagao, A. Samsudin, Proton (H+) transport properties of CMC–PVA blended polymer solid electrolyte doped with NH4NO3, International Journal of Hydrogen Energy, 45 (2020) 14880-14896.
[37] A. Samsudin, H. Lai, M. Isa, Biopolymer materials based carboxymethyl cellulose as a proton conducting biopolymer electrolyte for application in rechargeable proton battery, Electrochimica Acta, 129 (2014) 1-13.
[38] V. Hariharan, S. Radhakrishnan, M. Parthibavarman, R. Dhilipkumar, C. Sekar, Synthesis of polyethylene glycol (PEG) assisted tungsten oxide (WO3) nanoparticles for l-dopa bio-sensing applications, Talanta, 85 (2011) 2166-2174.
[39] J.J. Mittag, M.-L. Trutschel, H. Kruschwitz, K. Mäder, J. Buske, P. Garidel, Characterization of radicals in polysorbate 80 using electron paramagnetic resonance (EPR) spectroscopy and spin trapping, International Journal of Pharmaceutics: X, 4 (2022) 100123.
[40] M. Eikerling, A. Kornyshev, Proton transfer in a single pore of a polymer electrolyte membrane, Journal of electroanalytical chemistry, 502 (2001) 1-14.
[41] T. Ma, B. Li, S. Tian, J. Qian, L. Zhou, Q. Liu, B. Liu, X. Zhao, G. Sankar, Reversible photochromic W18O49: Mechanism revealing and performance improvement for smart windows, Chemical Engineering Journal, 468 (2023) 143587.
[42] H. Miyazaki, M. Inada, H. Suzuki, T. Ota, Molybdenum doping effects on photochromic properties of WO3 based composite films, Journal of the Ceramic Society of Japan, 121 (2013) 106-108.
[43] Q. Zhang, L. Xie, Y. Zhu, Y. Tao, R. Li, J. Xu, S. Bao, P. Jin, Photo-thermochromic properties of oxygen-containing yttrium hydride and tungsten oxide composite films, Solar Energy Materials and Solar Cells, 200 (2019) 109930.
[44] T. Sangpraserdsuk, M. Phiriyawirut, P. Ngaotrakanwiwat, J. Wootthikanokkhan, Mechanical, optical, and photochromic properties of polycarbonate composites reinforced with nano-tungsten trioxide particles, Journal of Reinforced Plastics and Composites, 36 (2017) 1168-1182.
[45] S. Songara, V. Gupta, M.K. Patra, J. Singh, L. Saini, G.S. Gowd, S.R. Vadera, N. Kumar, Tuning of crystal phase structure in hydrated WO3 nanoparticles under wet chemical conditions and studies on their photochromic properties, Journal of Physics and Chemistry of Solids, 73 (2012) 851-857.
[46] M. Bourdin, G. Salek, A. Fargues, S. Messaddeq, Y. Messaddeq, T. Cardinal, M. Gaudon, Investigation on the coloring and bleaching processes of WO 3− x photochromic thin films, Journal of Materials Chemistry C, 8 (2020) 9410-9421.
[47] R. Li, Y. Zhou, Z. Shao, S. Zhao, T. Chang, A. Huang, N. Li, S. Ji, P. Jin, Enhanced coloration/bleaching photochromic performance of WO3 based on PVP/PU composite matrix, ChemistrySelect, 4 (2019) 9817-9821.